Improved Productivity of NAD+ Reduction under Forced Convection in Aerated Solutions

Thi Xuan Huong Le, Julius Gajdar, Neus Vilà, Alain Celzard, Vanessa Fierro, Alain Walcarius, François Lapicque, Mathieu Etienne

Improved productivity of NAD^+ reduction under forced convection in aerated solutions

Thi Xuan Huong Le,[a] Julius Gajdar,[a] Neus Vilà,[a] Alain Celzard,[b] Vanessa Fierro,[b] Alain Walcarius,[a] François Lapicque,[c] Mathieu Etienne,[a,*]

[a] Université de Lorraine, CNRS, LCPME, F-54000, Nancy, France
[b] Université de Lorraine, CNRS, IJL, F-88000, Epinal, France
[c] Université de Lorraine, CNRS, LRGP, F-54000, Nancy, France

Abstract

The regeneration of the NADH cofactor is crucial for bioelectrocatalytic reactors. This can be achieved using an electrochemical mediator such as the rhodium complex $[Cp^*Rh(bpy)Cl]^+$, but the overall reduction process suffers from the interference of molecular oxygen. This interference can be avoided by using a second porous working electrode (acting as a real oxygen filter) positioned near the surface of the first working electrode. To fabricate the oxygen filter, platinum particles were deposited on the surface of a carbon paper. NADH could be produced in the presence of the oxygen filter with a faradaic yield at 63.4%, very close to the yields obtained without the filter at 61.7% in a fully N_2-degased medium, and only at 10.6% in the presence of oxygen. Moreover, the productivity was also increased by nearly a factor 4. Therefore, the proposed concept of the oxygen filter offers a new avenue in the current strategies for NADH regeneration in biocatalytic reactors based on electrochemical methods.

1. Introduction

The nicotinamide adenine (NADH) coenzyme is an important participant in a number of enzymatic processes. The redox processes involving NADH and NAD(P)H are significant from a biological and industrial perspective. The NAD/NADH couple mostly mediates transfer of protons and electrons in these processes. In order to decrease the cost of NADH in biosynthesis, its regeneration is needed. This study focuses on the electrochemical regeneration of NADH, but enzymatic, photochemical and chemical methods are also used [1]. The electrochemical regeneration offers low cost, easy process monitoring and straightforward product recovery [2]. The generated NADH can be used as a mediator in biocatalysis processes that are used in the synthesis of chemicals and pharmaceuticals [3], medicine [4] and biofuel industries [5].

Electrochemical regeneration of NADH involves the reduction of NAD^+ either directly on bare or modified electrodes or in the presence of redox mediators that facilitate this reduction. The electrochemical procedures to achieve NADH regeneration have been summarized in several recent reviews [2,6,7]. The direct reduction of NADH requires high overpotentials and is prone to produce biologically inactive forms of coenzyme [8]. Therefore, indirect forms of reduction using mediators are preferred. Recently, NADH regeneration was

reported with high efficiency on rhodium-based complexes with ligands such as bipyridine, polypyridine, pentamethylcyclopentadienyl, etc. [9–11]. In particular, a very effective mediator for NAD^+ reduction into biologically active NADH is the rhodium complex $[Cp^*Rh(bpy)Cl]^+$ [12–15]. Such mediator can be grafted onto bucky paper [16] electrodes, and can be used as an efficient immobilized catalyst for the transformation of $NAD(P)^+$ to NAD(P)H.

In all relevant cited works [9–11,15–17], dissolved oxygen has to be removed from the solution as oxygen reduction also occurs at negative operating potentials and therefore decreases the efficiency of the regeneration. This is usually carried out by purging the solution with an inert gas: nitrogen or argon, which is unpractical for many potential applications. Many deoxygenation systems have been designed based on chemical [18–21], enzymatic [22,23], or electrochemical methods [24,25]. Although presenting good efficiency, chemical and enzymatic methods related to oxygen scavenging showed a main disadvantage, namely the need to add reagent continuously to the reactor, or the limited duration of oxygen scavenging. Therefore, an electrochemical approach is considered in this study as a promising way to exclude this downside. This approach is based on the use of an additional porous electrode, placed in front of the working electrode, to which a negative potential is applied in order to electrochemically reduce oxygen before it can reach the working electrode surface. This idea was firstly investigated with a porous platinum electrode (platinum mesh) [26] that was applied for the detection of $NAD(P)^+$ in the absence of convection [27]. Electrochemical removal of oxygen was also shown for an electrochemical hydrazine sensor, in which an 80% reduction in oxygen response was observed using interdigitated platinum microelectrode array [28]. But detection is less critical than regeneration. Here, the challenge is finding a suitable material to operate efficiently with a higher mass transfer rate created by convection, which requires high surface area, good catalysis of the oxygen reduction reaction (ORR), and appropriate porosity, which should not hinder the diffusion of the analyzed molecules to the surface of the sensing electrode. This will also contribute to protect the electrocatalyst from oxygen, which is mandatory if interference of oxygen on NADH regeneration with $[Cp^*Rh(bpy)Cl]^+$ is to be avoided [29].

To improve the electrochemical performance of electrodes for ORR, catalysis by noble metals such as platinum has been usually applied as an efficient method. Oxygen is usually reduced directly to water as the main product on platinum; however, intermediates such as radicals or peroxides are also part of the reaction pathway [30,31]. In an effort to decrease the cost of materials for ORR catalysis, there has been a development of new materials based on cheaper metals and investigation of catalysis on nanoparticles [32]. Several methods for preparing electrodes based on platinum nanostructures that can noticeably catalyze ORR have been reported [33,34]. Promising results were achieved with a bimetallic PtNi-based catalyst prepared from the reduction of platinum(II) acetylacetonate ($[Pt(acac)_2]$) and nickel(II) acetylacetonate ($[Ni(acac)_2]$) using N, N-dimethylformamide (DMF) as both reducing agent and solvent, to grow octahedral PtNi on carbon supports [35]. Nevertheless, the preparation of the electrode necessitated a tedious process. In addition, the colloidal synthetic method used bulky capping agents like polymers, surfactants and/or fatty ligands for stabilization purposes, which

prevented the aggregation of the metallic nanocrystals during the preparation process [36,37]. In order to overcome the drawbacks associated with complicated synthesis procedures and reagents, a simple electrochemical method for growing platinum particles on a carbon electrode was reported. Platinum nanoparticles were directly deposited on a three-dimensional (3D) carbon felt electrode by an electrodeposition method [38]. This material showed enhanced stability and activity towards ORR.

In this study, we propose a simple, efficient and low-cost electrochemical oxygen filter, which can completely remove O_2 near the electrode under convection for the highly efficient regeneration of NADH. For this purpose, platinum particles were grown on the surface of a porous carbon paper (CP) for construction of the oxygen filter electrode via electrodeposition. The electrodeposition method was further optimized for ORR catalysis. The prepared electrode (Pt@CP) was characterized by physical techniques such as SEM, XRD and EDS. A modified bucky paper electrode (denoted BP-Bpy-Rh) prepared from multi-walled carbon nanotubes was fabricated by immobilization of $[Cp^*Rh(bpy)Cl]^+$ on its surface and then associated to the oxygen filter and employed for NADH regeneration in an aerated solution. The produced NADH was determined by UV spectrometry. The efficiency of the proposed oxygen filter was confirmed by repeating the same experiments after oxygen removal from the medium by nitrogen purging.

2. Results and discussion

2.1. Characterization of platinum particles on carbon paper electrode

2.1.1. Physical characterization

The direct growth of Pt particles on the surface of the CP electrode was achieved by electrodeposition using cyclic voltammetry in the Na_2PtCl_6 solution. The morphology of the as-fabricated Pt@CP was at first characterized by scanning electron microscopy. The result of the electrodeposition was a uniform dispersion of Pt nanoparticles onto the surface of the carbon paper (**Figure 1B and 1C)**. The result of EDS mapping (**Figure 1D**) confirmed that the platinum was successfully loaded onto the CP.

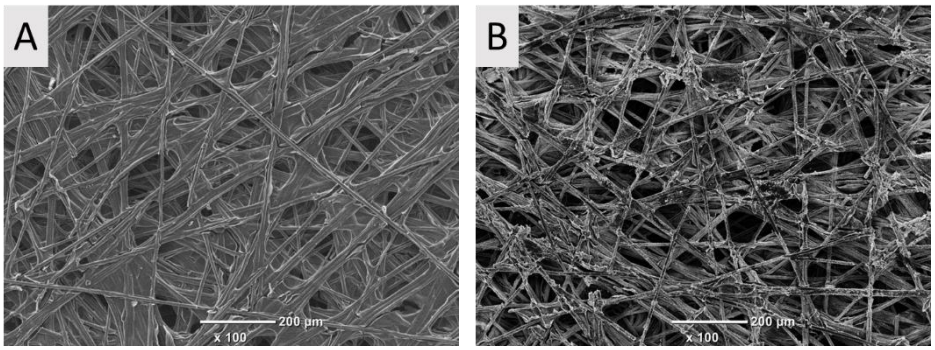

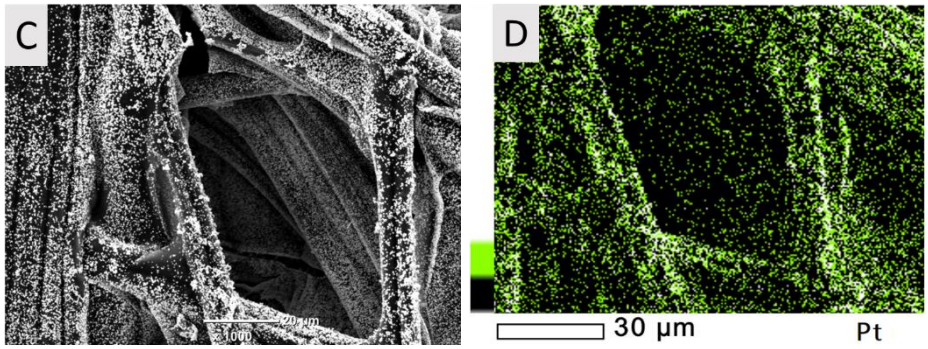

Figure 1. (A-C) SEM pictures of (A) carbon paper, CP, and (B) & (C) Pt@CP at different magnifications. (D) EDS mapping of Pt@CP.

The crystal structure of the modified electrode was characterized by XRD. The XRD patterns obtained for the carbon paper with and without Pt deposition are depicted in **Figure 2**. A broad diffraction line at 26.5° defined for the graphite crystal planes (002) and the smaller signal (004) at 54.7° were characteristic of raw CP [39]. The deposition of Pt on the carbon paper gave new diffraction lines located at 39.79°, 46.28°, 67.53°, 81.34° and 85.79°, corresponding to the (111), (200), (220), (311), and (222) planes, respectively, in agreement with previous reports [39, 40]. The crystallite size of Pt particles was estimated at approx.16 nm with an FWHM of 0.546° via the Scherrer equation (Eq. 1).

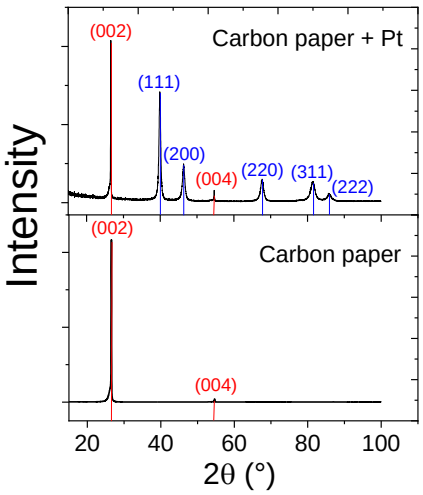

Figure 2. XRD spectra of carbon paper (bare CP) and Pt@CP.

2.1.2. Electrochemical characterization

The electrochemical behavior of the fabricated Pt@CP electrodes was compared to that of the raw CP by measuring their efficiency towards the oxygen reduction reaction (ORR) by CV (**Figure 3**). **Figure 3A** shows the CV of raw CP, Pt@CP and pure platinum electrode in 100 mM KCl solution at the scan rate of 5 mV s^{-1}. The peak corresponding to oxygen reduction was found around −0.7 V vs. Ag/AgCl for raw CP (see red curve). This peak was significantly shifted to a much less cathodic value, at approx. −0.1 V, with a two-fold increase in the peak current value when Pt particles were loaded onto the CP (see green curve), confirming an

improvement in catalytic performance by Pt modification. Additionally, the intense cathodic signal and the corresponding anodic peak appearing in the range between −0.7 V and −0.9 V are due to the proton reaction on the Pt-based material. This was confirmed by the control experiment performed with a solid bulky Pt electrode, giving rise to approximately the same behavior, but with oxygen reduction appearing at *ca.* –0.2 V (see blue curve), enabling to compare the ORR and the proton reaction with the Pt@CP electrode. When running the experiment with the Pt@CP electrode under nitrogen atmosphere, the oxygen reduction peak at –0.1 V was no longer visible **(Figure 3B)**, as expected, whereas the proton reduction process was still occurring.

In addition, the effect of the amount of platinum deposited on CP with respect to the ORR electrochemical performance was evaluated by investigating the influence of the concentration of $Na_2PtCl_6.6H_2O$ in the deposition solution. It is assumed that a higher concentration would result in a larger amount of Pt deposited on the carbon paper. The increase of Pt amount resulted in the progressive shift of the oxygen reduction peak towards the positive direction and the concomitant rise of peak current values (**Figure 3C)**. Moreover, the currents related to proton reduction (−0.7 V to −0.9 V) also increased proportionally to the Pt amount on CP. This confirms that Pt deposition also affected the catalytic H_2 production reactions, in agreement with previous observations [42]. There was no major improvement regarding the oxygen peak current or potential at a concentration higher than 0.94 mg mL^{-1}, which was therefore determined as the optimal value.

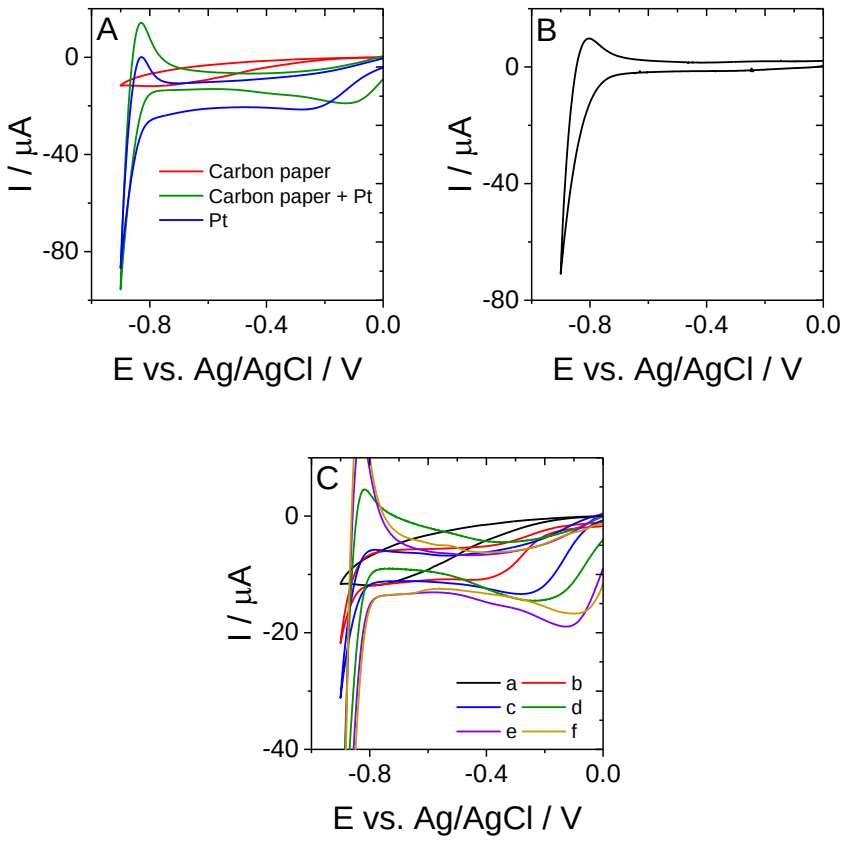

Figure 3. (A) CV of bare CP, Pt@CP, and pure Pt mesh, in the presence of dissolved oxygen, and (B) CV of Pt@CP under N_2. (C) CVs of dissolved oxygen recorded on Pt@CP prepared from solutions of $Na_2PtCl_6.6H_2O$ at various concentrations: 0.00 (*i.e.*, unmodified) (a); 0.12 (b); 0.24 (c); 0.47 (d); 0.94 (e); 1.88 (f) mg mL^{-1}. All measurements were performed in 100 mM KCl. The source of dissolved oxygen was ambient air. The scan rate of CVs was always 5 mV s^{-1}.

2.2. Pt@CP for oxygen filter under convection

The oxygen removal was performed in a four-electrode cell, including the platinum grid (counter electrode), a Ag/AgCl/1 M KCl (reference electrode), the glassy carbon (GCE, working electrode 1), and the Pt@CP or Pt grid (as oxygen filter and working electrode 2). It was confirmed in previous studies that applying a reduction potential (*i.e.*, −0.4 V) to the oxygen filter could completely eliminate oxygen interference in a static solution [26,27]. The absence of O_2 on GCE when operating under forced convection was checked by running CV from 0 V to −0.9 V at 5 mV s^{-1} in 100 mM KCl under stirring (800 rpm). As seen in **Figure 4A** (curve (c)), no signal of oxygen can be detected when using 2 layers of Pt@CP as an oxygen filter turned 'on'. On the contrary, the oxygen currents were nearly 60 times larger than the background ones after disconnecting the oxygen filter (curve (a)), due to the oxygen present in the solution. Therefore, the huge reduction current was observed around −0.6 V to −0.8 V vs. Ag/AgCl, which was assigned to ORR. Moreover, O_2 removal by using the oxygen filter based on Pt@CP was considerably more effective than a pure Pt grid (compare curves (b) and (c) in **Figure 4A**). The oxygen filter constructed from Pt grid could only decrease the oxygen concentration at the surface of GCE by about half of its value in the absence of the filter. This could be attributed to the large porosity of the structure of the Pt grid (0.04 mm wire diameter, 0.12 mm nominal space) as shown in **Figure S1** in Supporting Information. Consequently, oxygen molecules could still freely diffuse through the gaps between the Pt fibers, resulting in less effective O_2 removal with the Pt grid compared to the Pt@CP.

Furthermore, the effect of the number of Pt@CP layers on the O_2 elimination efficiency was also considered. First, the electrochemical performance towards the ORR of the oxygen filter consisting of one and two Pt@CP layers was investigated in a three-electrode cell (**Figure S2** in Supporting Information). As shown in part A of the figure, two combined Pt@CP layers as a working electrode showed a higher oxygen reduction current in a quiet solution, suggesting possible better performance for O_2 removal. This is confirmed in part B of the figure from experiments performed in a stirred medium. As shown, the oxygen reduction current decreased from 65 µA (in a case without an oxygen filter) to around 15 µA using one Pt@CP layer as the oxygen filter, which further decreased to 2 µA when placing two Pt@CP layers as the oxygen filter. Such performance could not be observed with two layers of the platinum grid.[43] To further prove the efficiency of the electrochemical filter for oxygen removal under convection, it was compared to an experiment performed under N_2 atmosphere (**Figure 4C**). It was noticed that the interference from oxygen molecules was completely eliminated at the filter, while

running a similar experiment under nitrogen atmosphere led to some residual currents that could be attributed to a minimal amount of O_2 still present in the solution after purging. This demonstrates the definite interest of using a Pt@CP electrode biased at a cathodic potential enabling the fast reduction of all the molecular oxygen initially present at the electrode/solution interface, and thus preventing any dissolved molecular O_2 from passing through the filter and reaching the surface of a sensing electrode. Nevertheless, a possible drawback of the method could be the measured electrochemical noise, higher with the filter than without filter.

Finally, the influence of the potential applied to the oxygen filter on the O_2 removal capacity was investigated by observing the oxygen reduction response on GCE during the application of different potential values from 0 V to −0.7 V *vs.* Ag/AgCl on the oxygen filter. The reduction current on GCE corresponding to ORR decreased significantly when increasing the cathodic potentials from 0 V up to −0.35 V at the oxygen filter as can be seen in **Figure 4B**. However, potentials more negative than −0.4 V did not further improve the efficiency with respect to O_2 elimination on GCE (and also led to noisier $I - t$ curves at the oxygen filter, see **Figure S3** in Supporting Information). Therefore, a potential in the range of −0.3 V to −0.4 V can be defined as a suitable choice to apply to the oxygen filter in these conditions.

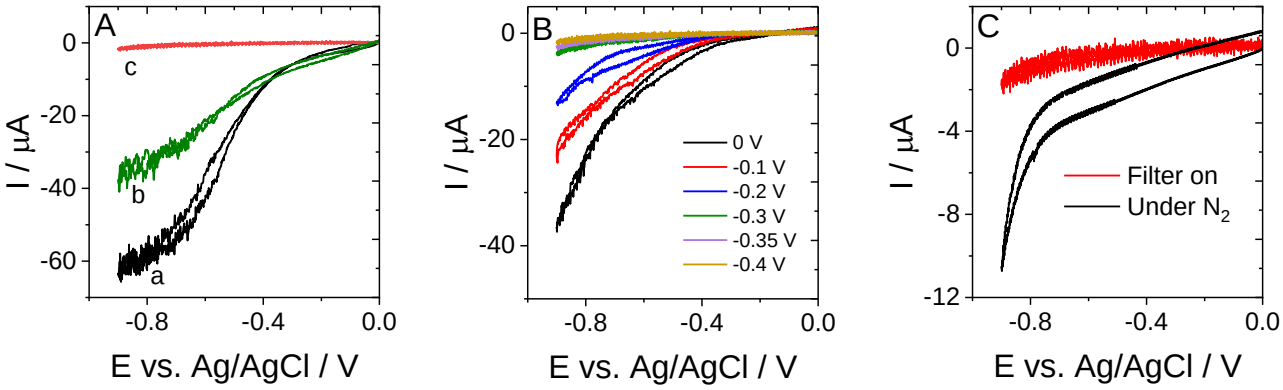

Figure 4. (A) CVs of oxygen reduction under convection on GCE in 100 mM KCl with (a) the oxygen filter 'off', (b) the filter 'on' using Pt grid filter (biased at −0.4 V), (c) and the filter 'on' using 2 layers of Pt@CP. (B) Effect of the applied potentials on Pt@CP on CV curves, and (C) comparison of the CV responses obtained when using the oxygen filter (Pt@CP biased at −0.4 V) or operating under N_2 in the absence of filter. The source of dissolved oxygen was ambient air. The scan rate was 5 mV s^{-1}.

2.3. Pt@CP filter for NADH regeneration under forced convection

The NADH regeneration reaction via the mediated electrochemical reduction of NAD^+ using rhodium-based electrocatalysts can be affected in the presence of oxygen because of the production of reactive oxygen species[29]. It therefore constitutes a good example to highlight one of the possible applications of the oxygen filter developed here for the rapid oxygen elimination by the Pt@CP electrode.

Bucky paper functionalized by rhodium complex (BP-Bpy-Rh) with a thickness of 35.3 µm (SEM image in **Figure S1** in Supporting Information), which was used for the mediated NAD^+ reduction, was placed as WE1. Two Pt@CP layers were kept unchanged as the oxygen filter (WE2) and biased at −0.4 V as above. Gradual NAD^+ concentrations were added to a stirred 10 mL solution of PBS (50 mM, pH = 6.5) during the chronoamperometric experiment with a potential of −0.78 V applied to WE1 (*i.e.*, a value likely to prevent hydrogen evolution and to enable the mediated NAD^+ reduction by $[Cp^*Rh(bpy)Cl]^+$, as determined from CV experiments[16,17]). The catalytic current increased linearly and levelled off at the concentration of 4 mM **(Figure 5A)**. Moreover, the catalytic current corresponding to 1 mM of NAD^+ was kept at the same level for more than 1 h in both cases of using the oxygen filter and working under N_2 atmosphere (**Figure 5B**). It was observed that the catalytic current when using the oxygen filter was more stable than N_2 bubbling (for which the currents tended to decrease with time), confirming the better performance for O_2 removal as discussed above (section 3.2, **Fig. 4C**). The amount of NADH produced by this process was estimated using UV-Vis spectroscopy, by monitoring the absorbance at 340 nm (**Figure 5C**). The evaluation of NADH production was carried out for three cases: (1) using the oxygen filter; (2) working under N_2 atmosphere; (3) operating in air without any oxygen removal strategy. The formed NADH was measured after 20 min of adding 4 mM NAD^+ to the PBS solution. NADH regeneration was significantly hindered due to the presence of O_2 at the surface of BP-Bpy-Rh when operating under air, resulting in the detection of only a small amount of NADH (see blue curve). Oxygen reduction intermediates and products can in this case interfere with NADH regeneration. On the contrary, the reduction product of ORR on platinum is mostly water [30,31] which should not hinder the regeneration. NAD^+ reduction occurred efficiently after removal of O_2, either by using the oxygen filter or by bubbling N_2 (see black and red curves). From these data, one can calculate faradaic efficiency values, which were 63.4 %, 61.7 % and 10.6 % when using the oxygen filter, working under N_2 atmosphere, or operating under the air, respectively (**Figure 5D**). In fact, the use of the oxygen filter can dramatically improve the faradaic efficiency (by ~50 %), which is comparable to the efficiency obtained in a nitrogen atmosphere. If one takes into account the current measured at the filter, the faradaic efficient drops to 35% which could appear less advantageous. But more important than the faradaic efficiency is the productivity. The overall amount of NADH produced by using the oxygen filter during this 20-minute regeneration was 0.46 µmol, which is 3-4 times increase over the value obtained under air (0.13 µmol). We interpret the low productivity observed in the presence of oxygen as being a consequence of the reactive oxygen species produced at the rhodium modified electrode degrading the catalyst, or the produced molecules or both.[44,45] This proves that the designed oxygen filter provides a stable catalytic current and offers excellent performance for bio-electrochemical applications without the need of taking care of oxygen removal by nitrogen bubbling.

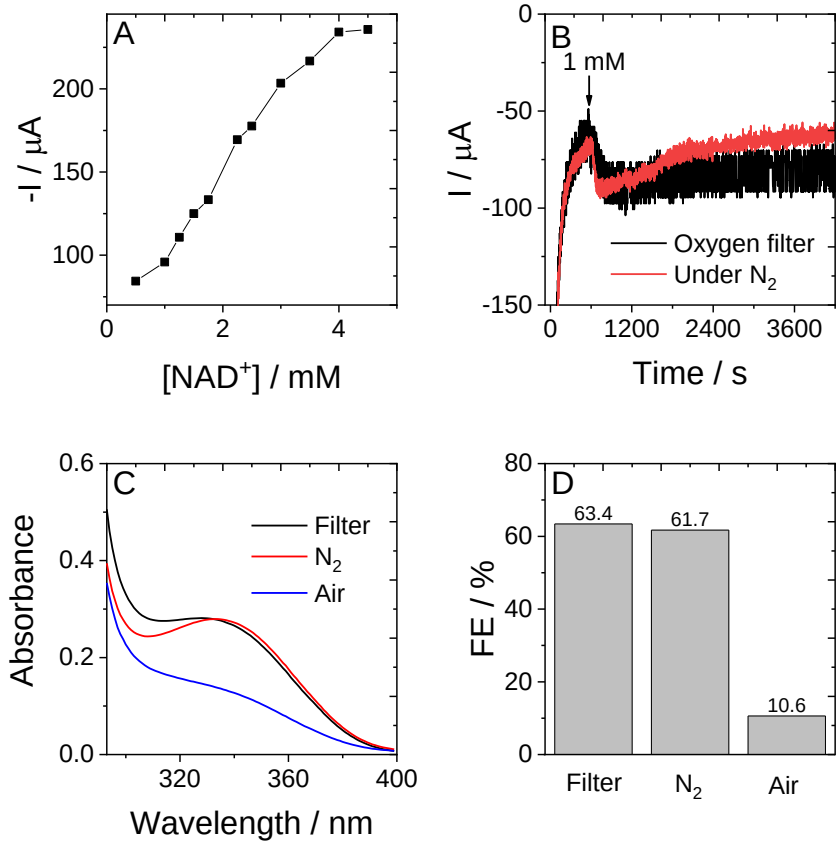

Figure 5. (A) Catalytic current obtained from chronoamperometry versus NAD^+ concentration recorded on BP-Bpy-Rh (WE1) in 50 mM PBS (pH = 6.5) at an applied potential of −0.78 V, using the oxygen filter (constructed from two layers of Pt@CP) biased at −0.4 V. (B) Comparison of amperometric responses recorded when using the oxygen filter (2 layers of Pt@CP) or under N_2 atmosphere, for 1 mM NAD^+ addition. (C) UV-vis spectra of NADH formed after 20 min by adding 4 mM of NAD^+ in the medium, as recorded after chronoamperometry experiments performed under air, nitrogen, or applying the oxygen filter. (D) Comparison of faradaic efficiency of NADH regeneration in these three conditions, as calculated from the data in (C). Stirring conditions were comparable for all experiments.

3. Conclusions

Platinum particles were successfully grown on the surface of a carbon paper electrode via electrochemical deposition by running CV in Na_2PtCl_6 solution (30 cycles from 0 V to −1 V *vs.* Ag/AgCl). The success of platinum deposition was confirmed by several characterization methods such as SEM, XRD and EDS. The electrochemical performance towards ORR was optimal in a plating solution containing 0.94 mg mL^{-1} of $Na_2PtCl_6.6H_2O$. The fabricated Pt@CP was used as a material for the construction of an oxygen filter in a four-electrode cell, likely to work under convective conditions. The oxygen interference was totally eliminated when using the oxygen filter formed by two stacked Pt@CP layers, operating at an applied potential of −0.4 V *vs.* Ag/AgCl. The O_2 removal capacity of this oxygen filter was demonstrated by comparing it with the same experiment performed under nitrogen atmosphere.

A possible application of this filter in a NAD^+/NADH regeneration case study was investigated by using a BP-Bpy-Rh modified electrode. It led to a faradaic efficiency value of 63.4 % when using the oxygen filter, a value nearly 6 times higher than that observed without any removal of dissolved oxygen. The total amount of NADH produced was nearly 4 times higher. In conclusion, Pt@CP proved to be an excellent material for the construction of an oxygen filter in order to completely remove oxygen from the surface of the working electrode, even under convection. The presented approach can be useful for applications in electrocatalysis, (bio)electrocatalytic reactors, or biosensing and it could also provide a protection for other O_2-sensitive catalysts. Further work should include stability assessment in combination with enzymatic systems.

Experimental

Chemicals and Materials

Carbon paper (CP, thickness 80 µm, CeTech GDS090) was bought from FuelCellStore. Glassy carbon (Sigradur) was provided by HTW Hoch-Temperatur-Werkstoffe (Germany). Nylon grid (39 µm wire diameter, 50 µm nominal space) and platinum grid (40 µm wire diameter, 120 µm nominal space) were purchased from Goodfellow SARL (France). Sodium hexachloro-platinate (IV) hexahydrate ($Na_2PtCl_6.6H_2O$, 98 %), β-nicotinamide adenine dinucleotide, reduced disodium salt hydrate (NADH, ≥ 97 %), β-nicotinamide adenine dinucleotide hydrate (NAD^+, ≥ 96.5 %), multi-walled carbon nanotubes (MWCNT, > 95 %, ∅ = 6-9 nm, L = 5 µm), 1 M hydrochloric acid solution, pentamethylcyclopentadienyl rhodium(III) chloride dimer ($(RhCp^*Cl_2)_2$) and potassium chloride (99.99 %) were obtained from Sigma-Aldrich. Sodium dihydrogen phosphate (99.5 %, Merck) and dichloromethane (Carlo Erba) were used without any purification. Aqueous solutions were prepared with high-purity water (18 MΩ cm) from a Purelab Option water purification system (Elga).

Electrodeposition of Pt on carbon paper electrode

The commercial CP was firstly cleaned in an ultrasonic bath containing an ethanol/H_2O mixture to eliminate any impurity resulting from the industrial manufacturing process. In addition, the cleaning step helped to reduce the hydrophobicity of the CP, which was necessary for Pt deposition in the next step. This pre-treated carbon paper was denoted as raw CP. Platinum was electrodeposited on the surface of raw CP by cyclic voltammetry, running 30 cycles from 0 V to −1 V (vs. Ag/AgCl) at a scan rate of 20 mV s^{-1} in a solution of 18.8 mg of $Na_2PtCl_6.6H_2O$ in 20 mL of 0.05 M phosphate buffer (pH = 6.5) under nitrogen atmosphere. The process was recorded on an Autolab (PGSTAT 100) using a three-electrode system with the raw CP as the working electrode, an Ag/AgCl/1 M KCl (Metrohm, Switzerland) reference electrode, and a platinum grid as the counter electrode. After the electrodeposition step, the sample was rinsed with deionized water and dried at 70 °C. The as-prepared sample was labelled Pt@CP.

Optimization of the use of Pt@CP for oxygen filter under convection

The oxygen filter system was composed of an electrochemical Teflon cylindrical cell with a round working area of 16.61 mm^2. It consisted of compacted Pt@CP (working electrode 2, WE2), Nylon separator, and glassy carbon (working electrode 1, WE1). An Ag/AgCl/1 M KCl reference electrode and a platinum grid as counter electrode were placed in a 100 mM KCl solution. In this system, WE2 acted as an oxygen filter that prevented dissolved O_2 molecules from reaching WE1. The experiment was performed under convection by stirring at a rate of 800 rpm. The presence of oxygen at the surface of WE1 was detected by running cyclic voltammetry from 0 V to −0.9 V (vs. Ag/AgCl) at a scan rate 5 mV s^{-1}, and applying a selected reduction potential at WE2. To evaluate the efficiency of the oxygen filter, various parameters were evaluated, including: the amount of Pt deposited on CP, the potential applied to WE2, and then the number of layers of Pt@CP. The oxygen removal effectiveness of the oxygen filter was checked by repeating the experiment under nitrogen atmosphere.

Application of the oxygen filter for NADH regeneration under convection

The oxygen filter was exploited to regenerate NADH in aerated solution. To perform this experiment, first, a bucky paper electrode (BP) was prepared from the dispersion of 10 g of MWCNT in 50 mL of ethanol by ultrasonication for 5 h. Then, the rhodium catalyst ($[Cp^*Rh(bpy)Cl]^+$) was immobilized on BP following the protocol reported in our previous publication [16]. The NAD^+ transformation was carried out by chronoamperometry at an applied potential of –0.78 V. Various amounts of NAD^+ were added gradually to the phosphate buffer solution (50 mM, pH = 6.5) to measure the catalytic current versus NAD^+ concentration recorded on the $[Cp^*Rh(bpy)Cl]^+$-functionalized bucky paper electrode (BP-Bpy-Rh). In this case, BP-Bpy-Rh was used as WE1 and Pt@CP was used as WE2, while the reference and counter electrodes remained the same as described in section 2.3. The concentration of generated NADH was determined by monitoring the absorbance at 340 nm by UV-Vis spectrometry. UV-Vis spectra were recorded on a Cary 60 Scan UV-Vis spectrophotometer. The NADH regeneration was repeated under nitrogen and air atmosphere (without using WE2) to compare the Faraday efficiency of the transformation.

Materials characterization

Chemical and structural characterizations were carried out by scanning electron microscopy (SEM, JEOL JCM-6000), X-ray diffraction (XRD, Panalytical X'Pert Pro diffractometer equipped with a Cu anticathode), and energy dispersive spectroscopy analysis (EDS, detector with Dx200s Digital Pulse Processor).

The crystallite size of Pt particles, *D* (Å), was obtained from the X-ray diffraction pattern using the Scherrer formula (Eq. 1) [46].

$$D = \frac{k\lambda}{\beta cos\theta} \qquad \text{(Equation 1)}$$

where k is a constant equal to 0.94, β (rad) is the full width at half maximum (FWHM) and λ (Å) is the X-ray wavelength.

Acknowledgements

This work was supported by the French PIA project "Lorraine Université d'Excellence", reference ANR-15-IDEX-04-LUE.

References

[1] S. Immanuel, R. Sivasubramanian, R. Gul, M. A. Dar, *Chem. – An Asian J.* **2020**, *15*, 4256–4270.
[2] C. Morrison, E. Heitmann, W. Armiger, D. Dodds, M. Koffas, *Adv. Appl. Microbiol.* **2018**, *105*, 51–86.
[3] R. A. Sheldon, D. Brady, M. L. Bode, *Chem. Sci.* **2020**, *11*, 2587–2605.
[4] P. Belenky, K. L. Bogan, C. Brenner, *Trends Biochem. Sci.* **2007**, *32*, 12–19.
[5] N. L. Akers, C. M. Moore, S. D. Minteer, *Electrochim. Acta* **2005**, *50*, 2521–2525.
[6] C. S. Morrison, W. B. Armiger, D. R. Dodds, J. S. Dordick, M. A. G. Koffas, *Biotechnol. Adv.* **2018**, *36*, 120–131.
[7] S. Kochius, A. O. Magnusson, F. Hollmann, J. Schrader, D. Holtmann, *Appl. Microbiol. Biotechnol.* **2012**, *93*, 2251–2264.
[8] A. Damian, K. Maloo, S. Omanovic, *Chem. Biochem. Eng. Q.* **2007**, *21*, 21–32.
[9] D. Sivanesan, S. Yoon, *Polyhedron* **2013**, *57*, 52–56.
[10] K. Vuorilehto, S. Lütz, C. Wandrey, *Bioelectrochemistry* **2004**, *65*, 1–7.
[11] F. Hollmann, B. Witholt, A. Schmid, *J. Mol. Catal. B Enzym.* **2002**, *19–20*, 167–176.
[12] E. Steckhan, S. Herrmann, R. Ruppert, J. Thömmes, C. Wandrey, *Angew. Chemie Int. Ed. English* **1990**, *29*, 388–390.
[13] R. Ruppert, S. Herrmann, E. Steckhan, *J. Chem. Soc. Chem. Commun.* **1988**, 1150–1151.
[14] R. Ruppert, S. Herrmann, E. Steckhan, *Tetrahedron Lett.* **1987**, *28*, 6583–6586.
[15] E. Steckhan, S. Herrmann, R. Ruppert, E. Dietz, M. Frede, E. Spika, *Organometallics* **1991**, *10*, 1568–1577.
[16] L. Zhang, M. Etienne, N. Vilà, T. X. H. Le, G.-W. Kohring, A. Walcarius, *ChemCatChem* **2018**, *10*, 4067–4073.
[17] A. Walcarius, R. Nasraoui, Z. Wang, F. Qu, V. Urbanova, M. Etienne, M. Göllü, A. S. Demir, J. Gajdzik, R. Hempelmann, *Bioelectrochemistry* **2011**, *82*, 46–54.
[18] S. Kikuchi, K. Honda, S. Kim, *Bull. Chem. Soc. Jpn.* **1954**, *27*, 65–68.
[19] D. Quan, J. N. Shim, J. D. Kim, H. S. Park, G. S. Cha, H. Nam, *Anal. Chem.* **2005**, *77*, 4467–4473.
[20] Y. Gu, C. C. Chen, *Sensors* **2008**, *8*, 8237–8247.
[21] K. Andersen, T. Kjar, N. P. Revsbech, *Sensors Actuators, B Chem.* **2001**, *81*, 42–48.
[22] N. Plumeré, J. Henig, W. H. Campbell, *Anal. Chem.* **2012**, *84*, 2141–2146.
[23] M. Swoboda, J. Henig, H. M. Cheng, D. Brugger, D. Haltrich, N. Plumeré, M. Schlierf, *ACS Nano* **2012**, *6*, 6364–6369.
[24] N. Plumeré, *Anal. Bioanal. Chem.* **2013**, *405*, 3731–3738.
[25] A. Prévoteau, N. Mano, *Electrochim. Acta* **2012**, *68*, 128–133.
[26] M. Etienne, T. X. H. Le, T. Nasir, G. Herzog, *Anal. Chem.* **2020**, *92*, 7425–7429.
[27] T. X. H. Le, M. Etienne, F. Lapicque, A. Hehn, N. Vilà, A. Walcarius, *Electrochim. Acta* **2020**, *353*, 136546.
[28] E. Bertin, S. Garbarino, D. Guay, *Electrochem. commun.* **2016**, *71*, 56–60.

[29] A. Tosstorff, A. Dennig, A. J. Ruff, U. Schwaneberg, V. Sieber, K. M. Mangold, J. Schrader, D. Holtmann, *J. Mol. Catal. B Enzym.* **2014**, *108*, 51–58.
[30] V. Briega-Martos, E. Herrero, J. M. Feliu, *Electrochim. Acta* **2017**, *241*, 497–509.
[31] A. M. Gómez-Marín, J. M. Feliu, E. Ticianelli, *ACS Catal.* **2019**, *9*, 2238–2251.
[32] L. Liu, A. Corma, *Chem. Rev.* **2018**, *118*, 4981–5079.
[33] A. Chen, P. Holt-Hindle, *Chem. Rev.* **2010**, *110*, 3767–3804.
[34] R. Devivaraprasad, N. Nalajala, B. Bera, M. Neergat, *Front. Chem.* **2019**, *7*, 648.
[35] X. Huang, Z. Zhao, Y. Chen, E. Zhu, M. Li, X. Duan, Y. Huang, *Energy Environ. Sci.* **2014**, *7*, 2957–2962.
[36] C. Cui, L. Gan, M. Heggen, S. Rudi, P. Strasser, *Nat. Mater.* **2013**, *12*, 765–771.
[37] J. Zhang, H. Yang, J. Fang, S. Zou, *Nano Lett.* **2010**, *10*, 638–644.
[38] W. E. Kosimaningrum, T. X. H. Le, Y. Holade, M. Bechelany, S. Tingry, B. Buchari, I. Noviandri, C. Innocent, M. Cretin, *ACS Appl. Mater. Interfaces* **2017**, *9*, 22476–22489.
[39] T. X. H. Le, M. Bechelany, A. B. Engel, M. Cretin, S. Tingry, *Electrochim. Acta* **2016**, *219*, 121–129.
[40] J. Yu, T. Dai, Y. Cao, Y. Qu, Y. Li, J. Li, Y. Zhao, H. Gao, *J. Colloid Interface Sci.* **2018**, *524*, 360–367.
[41] J. Zhang, W. Chen, H. Ge, C. Chen, W. Yan, Z. Gao, J. Gan, B. Zhang, X. Duan, Y. Qin, *Appl. Catal. B Environ.* **2018**, *235*, 256–263.
[42] M. Monai, T. Montini, E. Fonda, M. Crosera, J. J. Delgado, G. Adami, P. Fornasiero, *Appl. Catal. B Environ.* **2018**, *236*, 88–98.
[43] E. Rotureau, J. Gajdar, G. Herzog, Y. Waldvogel, J. P. Pinheiro, M. Etienne, *Anal. Chim. Acta* **2021**, *1167*, 338544.
[44] L. Castañeda-Losada, D. Adam, N. Paczia, D. Buesen, F. Steffler, V. Sieber, T. J. Erb, M. Richter, N. Plumeré, *Angew. Chemie - Int. Ed.* **2021**, *60*, 21056–21061.
[45] H. Li, U. Münchberg, A. A. Oughli, D. Buesen, W. Lubitz, E. Freier, N. Plumeré, *Nat. Commun.* **2020**, *11*, 1–7.
[46] T. X. H. Le, C. Charmette, M. Bechelany, M. Cretin, *Electrochim. Acta* **2016**, *188*, 378–384.

Table of Contents

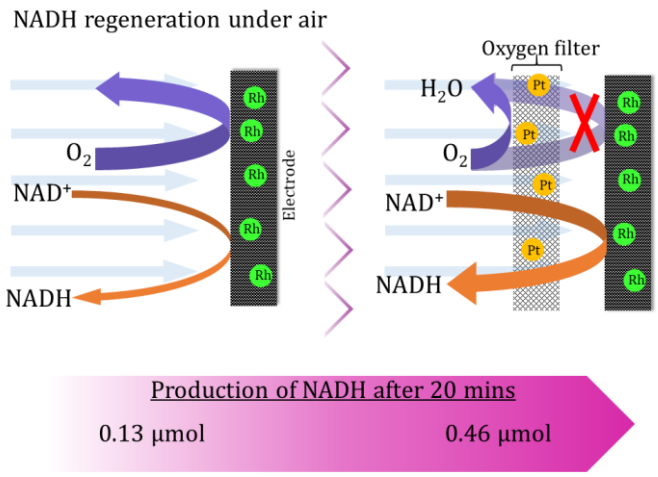

The interference of oxygen on electrochemical regeneration of NADH in aerated solutions was removed using electrochemical oxygen filter which was prepared by deposition of Pt nanoparticles on carbon paper. The filter successfully removed oxygen molecules in the vicinity of the working electrode under convective conditions.

Keywords: coenzyme regeneration, electrochemical oxygen filter, NADH, oxygen reduction reaction